International Journal of Thermophysics (2024) 45:70
https://doi.org/10.1007/s10765-024-03363-x

Prediction of Greenhouse Gas Solubility in Eutectic Solvents Using COSMO-RS

Fernanda Paludetto Pelaquim[1] · Sérgio M. Vilas-Boas[1] · Débora Costa do Nascimento[1] · Pedro J. Carvalho[2] · Antonio Marinho Barbosa Neto[3] · Mariana Conceição da Costa[1]

Received: 11 March 2024 / Accepted: 26 March 2024

Abstract
Over the past few years, eutectic solvents (ESs) have drawn the scientific community's attention because they are usually more environmentally friendly than traditional organic solvents. One of the applications of ESs is in the gas capture field, where they are considered promising absorbers to replace amine- (MEA, DEA, or MDEA processes), methanol- (Rectisol process), dimethyl ethers of polyethylene glycol- (Selexol process), *N*-methyl-2-pyrrolidone- (Purisol process), propylene carbonate- (Fluor solvent process), or morpholine-based (Morphysorb process) solvents on CO_2 capture from the atmosphere. Although several studies have reported experimental gas solubility data in ESs, especially for CO_2, only a few existing options are covered. In fact, resorting to experimental methods to obtain the solubility data seems unfeasible considering the vast number of possible eutectic mixtures. Therewith, theoretical predictions of gas solubility in ESs are valuable for the fast prescreening of prospective solvents. In this work, the ability of the thermodynamic model COSMO-RS to represent solubility data of CO_2, CH_4, and H_2S in 17 choline chloride-based (ChCl) ESs was evaluated. The experimental data were collected from the literature at different molar ratios, at 298.15 K or 313.15 K, and in the pressure range from 1 to 125 bar. COSMO-RS offers a qualitative description of these gases' solubility, which was expected due to the model's fully predictive character. To improve the CO_2 and CH_4 solubility data description, a temperature–pressure-dependent correction was applied to the COSMO-RS predictions for these gases, offering a global average relative deviation of 15%.

Keywords Carbon dioxide · COSMO-RS · Eutectic solvents · High pressure · Methane · Solubility

Extended author information available on the last page of the article

Published online: 16 April 2024

1 Introduction

The increasing evidence of an imminent global and systemic environmental crisis has led the scientific community to develop more sustainable products and processes [1]. In this context, green chemistry has emerged as one of the main topics in chemistry, aiming to create products and processes to reduce or eliminate the use and generation of hazardous substances [2]. One of the major green chemistry issues is replacing traditional organic solvents, usually volatile and toxic, for more sustainable options, the so-called alternative solvents, such as eutectic solvents (ESs) [3].

A eutectic mixture is often defined as a mixture of components that, at fixed proportions, have a melting temperature lower than the melting points of the pure compounds [4, 5]. The term deep eutectic solvent (DES) is often attributed to eutectic mixtures formed by at least two components, a hydrogen bond donor (HBD) and a hydrogen bond acceptor (HBA), with a eutectic point temperature (and a solid–liquid phase behavior) below that of an ideal liquid mixture, as reported by Martins and coworkers [6]. Otherwise, the mixture can be called simply a eutectic solvent (ES), which is observed for most systems reported in the literature.

Studies show that ESs might present environmental, economic, and technological advantages over traditional organic solvents [7] due to their low prices, low vapor pressure, nonflammability, biocompatibility, biodegradability, and easy preparation processes [8–11]. Consequently, both DESs and ESs have received great attention in recent decades due to their potential to replace organic solvents in various applications, such as media for extracting and purifying biocompounds [12], hydrate inhibitors [13, 14], metal processing and metal decomposition agents [15–17], two-phase aqueous system forming agents [18, 19], and gas capture media [20–22].

Regarding gas capture, the continuous increase in fossil fuel usage for transportation and electricity, along with land misuse and other human activities, have led to excessive greenhouse gas (GHG) emissions, especially carbon dioxide (CO_2) [23, 24]. According to the International Energy Agency (IEA) global energy review on CO_2 emission in 2021 [25], global energy-related CO_2 emissions rose by 6%, corresponding to 36.3 billion tons of CO_2 released to the atmosphere, the largest registered level in history in absolute terms up to 2021. Nonetheless, mitigating GHG emissions is mandatory because of their negative effects on climate change [26]. The most effective action toward reducing CO_2 emissions would involve replacing fossil fuels with renewable energy sources. However, fossil-fuel-based power plants remain the most viable process for electricity and power generation due to their lower price [27, 28]. Under these circumstances, technologies aiming to capture flue gases seek to offer a pragmatic approach to reducing emissions in the coming years [29].

Developing strategies such as CO_2 capture, utilization, and storage (CCUS) technology could greatly contribute to reducing CO_2 emissions. These technologies can be divided into precombustion, oxyfuel combustion, and post-combustion capture [23, 30, 31]. The latter is a suitable alternative to reduce CO_2 emissions in coal-fired power plants [23]. In post-combustion technology, CO_2 is separated from the flue gases through absorption, membrane separation, adsorption, or a combination of these technologies [32, 33]. Alternatively, amine-based (such as MEA, DEA, or MDEA) aqueous solutions have traditionally been used as chemical solvents to capture CO_2 due to their excellent absorption capacity, high reactivity, high selectivity, and low price. However, amine-based processes may undergo solvent loss or degradation, equipment corrosion, and volatile organic compounds (VOCs) emission. Regarding physical absorption, which is the case of most ESs, Selexol is a commercial process that uses dimethyl ether of polyethylene glycol (DEPG) as a solvent, and it is applied for the selective removal of hydrogen and CO_2. This solvent presents low vapor pressure, chemical and thermal stability, and a non-corrosive and non-toxic nature; however, the high solubility of DEPG increases the pumping cost. These drawbacks have propelled the development of new materials for CO_2 capture, such as ESs [34–37].

The efficiency of different ESs in physically absorbing CO_2 has been mainly addressed over the years by evaluating experimental CO_2 solubility in the liquid phase [20, 24, 38–40]. Nevertheless, almost infinite possibilities of HBA and HBD combinations can result in ESs, and performing experimental solubility studies in all cases becomes unfeasible. Thus, theoretical predictions of CO_2 solubility in ESs are recommended for a fast pre-screening of prospective solvents [41, 42]. In recent studies, classical thermodynamic models such as the Non-Random Two-Liquid (NRTL) model [21, 43] or equations of state, such as PC-SAFT, Cubic Plus Association (CPA), and Peng–Robinson (PR) [44–48], paired with the equilibrium isofugacity criteria, have been successfully used to describe gas solubility in organic solvents and ESs.

Although the models mentioned above often deliver good representations of the solubility data, they are semi-empirical approaches that require experimental thermophysical data, such as density, vapor pressure, and heat capacity, to fit the model's parameters. Unfortunately, these data are not easily found in the literature for ESs [42, 46]. More predictive models, such as the Conductor-like Screening Model for Real Solvents (COSMO-RS) [49–51], arise as attractive tools to describe the phase behavior of systems lacking experimental thermophysical data. COSMO-RS has shown to be useful for solvent screening purposes [52–54] due to its predictive nature with a qualitative accuracy [24, 49]. The model estimates the thermodynamic equilibria of fluids using a statistical thermodynamic approach combined with quantum chemical calculations.

Despite the topic's relevance, only a few studies aiming at modeling CO_2 solubility in ESs have been reported [24, 41–43, 55–60]. In this context, this work aims to evaluate the potentialities of COSMO-RS in describing the solubility of three greenhouse gases, CO_2, CH_4, and H_2S, in different ESs. An experimental solubility database of the three selected gases in different ESs was built from data available in the literature. Then, the COSMO-RS model was applied to describe the solubility data, and the model's performance was compared with the results achieved with more empirical thermodynamic approaches reported in previous studies, such as the PC-SAFT, CPA, and Peng–Robinson equations of state [46]. Finally, a temperature–pressure-dependent correction is proposed to refine the COSMO-RS predictions, improving the CO_2 and CH_4 solubility predictions in the studied ESs.

2 Materials and Methods

2.1 Eutectic Solvent Database Collection

Experimental gas solubility data in ESs were collected from the literature. A database comprising the compounds' molecular structure and polarization charge density (cosmo file) was built, allowing us to infer the COSMO-RS predictive accuracy. In this study, 208 solubility data points of CO_2, CH_4, and H_2S in 17 different ESs, at 313.15 K and pressures varying from 1 to 125 bar, were gathered from the literature. All these data are compiled in Table 1.

Choline chloride was chosen as the common HBA, and 15 HBDs were selected, including ethylene glycol, glycerol, phenol, urea, 1,4-butanediol, 2,3-butanediol, 1,2-propanediol, diethylene glycol, triethylene glycol, levulinic acid, furfuryl alcohol, guaiacol, lactic acid, malonic acid, and phenylacetic acid. The HBA:HBD molar ratios of 1:2, 1:3, and 1:4 were considered for CO_2 solubility calculation, while the molar ratio of 1:1 was considered for CH_4 calculation due to the scarcity of experimental data. The only exception was for the ES composed of ChCl (HBA) and urea (HBD), where HBA:HBD molar ratios equal to 1:1.5, 1:2, and 1:2.5 were studied.

Table 1 ChCl-based ESs molar ratio, gas solubility range, and pressure range of the systems analyzed in this study

Gas	HBD	Molar ratio (HBA:HBD)	Pressure range (bar)	Gas solubility (x_1)	References
CO_2	Ethylene Glycol	1:2	2.48–59.02	0.008–0.230	[61]
CO_2	Glycerol	1:2	1.91–59.91	0.019–0.331	[62]
CO_2	Phenol	1:2; 1:3; 1:4	1.16–127.40	0.003–0.275	[63, 64]
CO_2	Urea	1:1.5; 1:2; 1:2.5	10.70–125.00	0.046–0.309	[65, 66]
CO_2	1,4−butanediol	1:3; 1:4	1.12–5.07	0.003–0.012	[67]
CO_2	2,3−butanediol	1:3; 1:4	1.11–5.29	0.003–0.014	[67]
CO_2	1,2−propanediol	1:3; 1:4	1.21–5.25	0.002–0.012	[67]
CO_2	Diethylene Glycol	1:3; 1:4	1.16–5.18	0.003–0.015	[64]
CO_2	Triethylene Glycol	1:3; 1:4	1.14–5.19	0.004–0.020	[64]
CO_2	Levulinic acid	1:3; 1:4	0.60–5.80	0.003–0.027	[68]
CO_2	Furfuryl alcohol	1:3; 1:4	0.70–5.82	0.002–0.018	[68]
CO_2	Guaiacol	1:3; 1:4	0.53–5.43	0.001–0.016	[34]
CH_4	Lactic acid	1:1	0.05–49.93	0.004–0.287	[69]
CH_4	Malonic acid	1:1	0.05–49.93	0.004–0.281	[69]
CH_4	Phenylacetic acid	1:1	0.05–49.92	0.005–0.0322	[69]
CH_4	Urea	1:1.5; 1:2; 1:2.5	0.10–2.03	4E-05–0 001	[66]
H_2S	Urea	1:1.5; 1:2; 1:2.5	0.10–2.02	0.002–0.055	[66]

2.2 COSMO-RS

The COSMO-RS is a predictive model that combines the dielectric continuum solvation model, known as COSMO, and statistical thermodynamics [49]. Hereupon, COSMO-RS uses the interaction between a cavity containing a molecule and a dielectric media, generated through quantum chemistry Density Functional Theory (DFT)-based calculations, as a reference state from which interaction energies between molecules can be inferred [51]. Through statistical thermodynamics, the definition of an ensemble of pairwise small surface segments of different molecules interacting with each other, along with the establishment of a partition function from which the Gibbs energy of the system can be derived, enables the calculation of solution properties from COSMO-RS [51].

In fact, the contact between molecules in the reference state of COSMO causes the appearance of interaction energies, which contribute to the overall Gibbs energy. It is possible to derive chemical potentials from the Gibbs energy, thus allowing COSMO-RS to calculate thermodynamic equilibria. The model, in essence, depends only on the molecule's geometry and polarization charge density to determine equilibrium conditions for multicomponent systems, which is a notable advantage over empirical or semi-empirical approaches. To describe the vapor–liquid phase diagram at a fixed pressure (isobaric) or fixed temperature (isothermal), the activity coefficient model computes a list of concentrations that cover the whole range of mole fractions of the system and calculates the excess enthalpy and Gibbs free energy, the species chemical potentials and activity coefficients, the total vapor pressure of the system, and the concentrations of the species in the gas phase. The total pressure of the system is obtained using the modified Raoult's law:

$$p = \sum_i p_i^{\sigma} x_i \gamma_i. \tag{1}$$

COSMO-RS assumes ideal behavior in the gas phase, being the species vapor mole fractions obtained from the ratio of the total pressure and partial vapor pressures.

$$p_j = p_j^{\sigma} x_j \gamma_j, \tag{2}$$

$$y_i = \frac{p_i^{\sigma} x_i \gamma_i}{p}, \tag{3}$$

where p_j^{σ} and γ_j are the vapor pressure and the activity coefficient of component j, respectively.

In the present work, the COSMOtherm software (version 21.0) [70] with the BP_TZVPD_FINE_21.ctd level of parametrization was used to estimate the solubility data of the greenhouse gases in the eutectic mixtures. All the required cosmo files for the gases and some ES precursors (phenol, ethylene glycol, and glycerol) were retrieved from the COSMOtherm TZVPD-FINE database. For ChCl and all the HBD missing in the database, the input files were obtained with the COSMOconfX 2021 software coupled to the TmoleX (version 4.5) package using the

BP-TZVPD-FINE-COSMO + GAS_18 template [71]. ChCl was treated following the electroneutral mixture approach [72]. Additional details for the gas solubility calculation procedure with COSMOtherm are available in the software reference manual [73]. Moreover, all conformers available for each molecule were considered in the simulations.

3 Results and Discussion

The solubilities predicted with COSMO-RS were compared against the experimental data presented in Table 1, which includes the solubility of CO_2, CH_4, and H_2S in 17 different ESs with various HBA:HBD molar ratios (1:1, 1:1.5,1:2, 1:2.5, 1:3 and 1:4), at 313.15 K and pressures ranging from 1 to 125 bar. The Average Relative Deviation (ARD) for each *pTx* dataset was calculated according to Eq. 4 to evaluate the COSMO-RS capability to describe the experimental data.

$$\mathrm{ARD} = \frac{1}{N_\mathrm{p}} \sum_{i=1}^{N_\mathrm{p}} \frac{\left| x_i^{\mathrm{exp}} - x_i^{\mathrm{cal}} \right|}{x_i^{\mathrm{exp}}}, \tag{4}$$

where N_p is the number of experimental data, i is the analyzed gas (CO_2, CH_4, and H_2S), x_i^{exp} is the experimental gas solubility, and x_i^{cal} is the gas solubility calculated with COSMO-RS.

All the 208 experimental data points were plotted against the predicted results (further discussed in the following sections), and the corresponding ARDs are listed in Tables S1–S33 of the Supplementary Information (SI). Also, experimental pressure–solubility curves are compared with those predicted with COSMO-RS in Figs. S1–S4 of the SI for many of the studied systems to support the discussion presented in the following sections.

3.1 CO_2 Solubility in ESs at 1:2 (ChCl:HBD) Molar Ratio

The experimental and predicted solubility data of CO_2 in ESs at 1:2 HBA:HBD molar ratio are depicted in Fig. 1. For all of these ESs, COSMO-RS could qualitatively describe the experimental data, presenting ARDs varying between 26% and 81%. Although COSMO-RS underestimated the solubilities of all ESs, except ChCl:Ethylene Glycol, the model provided similar curve trends as those reported in the literature [61].

The best results were obtained for the ESs containing diols as the HBD, the ChCl:Glycerol (ARD = 26%) and ChCl:Ethylene glycol (ARD = 34%), while higher deviations were observed for ChCl:Urea (58%) and ChCl:Phenol (ARD = 81%). For example, the experimental CO_2 solubility data, x_{CO2}, in ChCl:Glycerol was 0.310 at 313.15 K and 59.91 bar, and the COSMO-RS predicted value was 0.285, corresponding to an ARD of 14%. In contrast, the experimental CO_2 solubility in ChCl:Phenol at the same temperature and 64.5 bar was

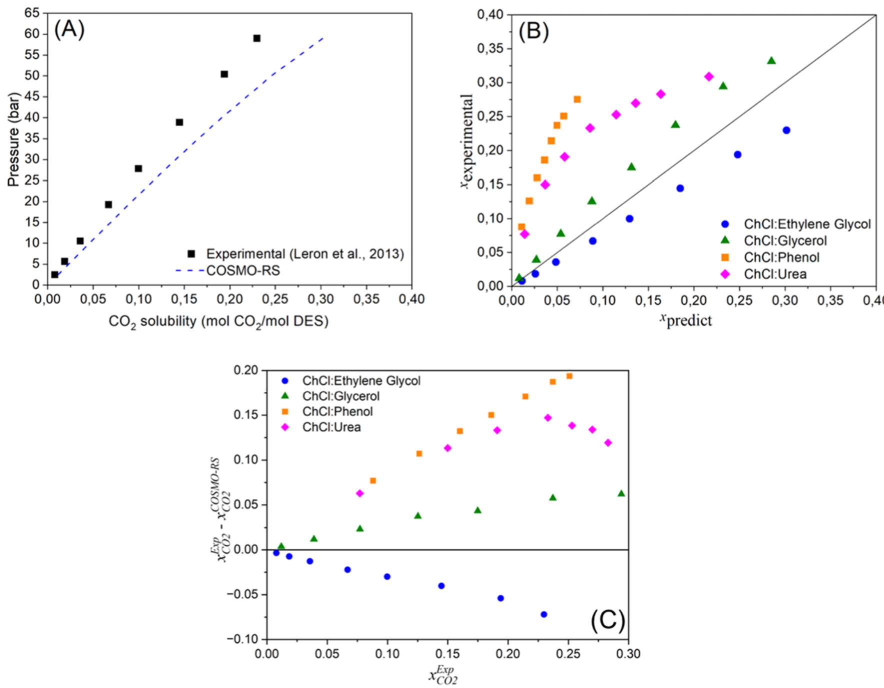

Fig. 1 (A) Comparison of the experimental and predicted CO_2 solubility in ChCl:Ethylene glycol (at 1:2 HBA:HBD molar ratio); (B) experimental x_{CO2} vs. x_{CO2} predicted with COSMO-RS for all studied ESs at 1:2 molar ratio; (C) solubility differences as function of the experimental CO_2 solubility values

0.186, about five times the value predicted with COSMO-RS (x^{cal}_{CO2}= 0.036). In most cases, the COSMO-RS predictions are more qualitative, meaning they can distinguish the best solvents from the worst ones, as shown in Fig. 1(C).

The experimental CO_2 solubility ranks as ChCl:Glycerol > ChCl:Ethylene Glycol ≈ ChCl:Urea > ChCl:Phenol. Since the HBA is the same for all ESs, the difference between the CO_2 solubility values is attributed to the HBDs. As glycerol has a longer chain length than ethylene glycol and urea, and it has more hydroxyl groups than the other HBDs, the free volume of the ES containing this molecule is the highest [46]. Consequently, there is more free space for CO_2 hosting in glycerol-based ES than in the others. Although the solubility rank obtained with COSMO-RS is slightly different from the experimental trend (ChCl:Glycerol ≈ ChCl:Ethyelene Glycol > ChCl:Urea > ChCl:Phenol), the model identifies ChCl:Phenol as the ES with the least solubilization capacity, while confirming that the ESs containing the diols as HBD solubilize more CO_2.

Figure 1(A) compares the CO_2 solubility in ChCl:Ethylene glycol and the COSMO-RS predictions. As can be seen, the experimental CO_2 solubility values increase as the pressure increases; COSMO-RS also describes this behavior well. Similar trends were observed for the other studied ESs. This result is even more evident for ChCl:Urea and ChCl:Phenol, which exhibit experimental CO_2 solubility up to 130 bar. These large deviations seen in Fig. 1 were an expected outcome

Table 2 Comparison of the deviations between the experimental and calculated solubilities with COSMO-RS (this work) and CPA and Peng–Robinson EoSs [46]

HBA	HBD	Pressure (bar)	%ARD in x for COSMO-RS[a]	%ARD in x for Peng–Robinson	%ARD in x for CPA
ChCl	Ethylene Glycol	26.80–27.80	33.81	17.23	2.79
ChCl	Glycerol	27.60–29.78	25.64	5.15	5.92
ChCl	Urea	28.50–29.20	58.31	5.94	2.45

as COSMO-RS assumes liquid state's incompressibility and gas phase's ideality, computing only pressure-independent activity coefficients, and not fugacity coefficients. To improve the prediction results for high-pressure systems, Moity et al. [74] emphasize the need to combine COSMO-RS and an equation of state (EoS).

Liu et al. [41] also predicted the CO_2 solubility in ChCl:Phenol at 313.15 K and low pressures (between 1.22 and 5.03 bar) using COSMO-RS (with the BP_TZVP_C30_1401 level of parametrization). The authors obtained solubility predictions one order of magnitude higher than the experimental data, resulting in ARDs much higher than those obtained in this work. It is also possible to compare the results of this work with those obtained in our previous study [46], where the Cubic Plus Association (CPA) and Peng–Robinson equations of state (EoSs) were applied to model the CO_2 solubility in ESs. In our previous work, the ESs were modeled as individual components, as shown in Table 2, and adjusted the binary interaction parameters (k_{ij}). Both EoSs (CPA and Peng–Robinson) offer a better description of the CO_2 solubility in the three ESs than COSMO-RS (Table 2), which is expected due to the fully predictive nature of COSMO-RS.

3.2 CO_2 Solubility in ESs at 1:3 and 1:4 Molar Ratios

Figures 2 and 3 compare the experimental and predicted CO_2 solubility (with COSMO-RS) in 9 ESs at 1:3 and 1:4 molar ratios, at 313.15 K and pressures ranging from 0.50 to 6.00 bar, respectively. The ARDs between the experimental and the predicted solubility values are presented in Tables S8–S25 and Figure S2 and S3 of the SI. In these cases, COSMO-RS notably overpredicted the CO_2 solubilities, achieving ARDs between 51% (ChCl:Levulinic acid, at 1:4) and 303% (ChCl:Guaiacol, at 1:3). The experimental CO_2 solubility data in these ESs are much lower compared to the solubility in the same ESs at 1:2 molar ratio presented in Sect. 3.1 (at similar pressure ranges), and COSMO-RS does not fully capture these trends.

Three factors influence the deviation between experimental data and those predicted by COSMO-RS: pressure, temperature, and the molar ratio [75]. Higher relative deviations are observed at lower pressures. On the other hand, the molar ratio causes a reduction of the deviations in almost all mixtures, especially for ChCl:Levulinic Acid (from 111.32% to 51.04%).

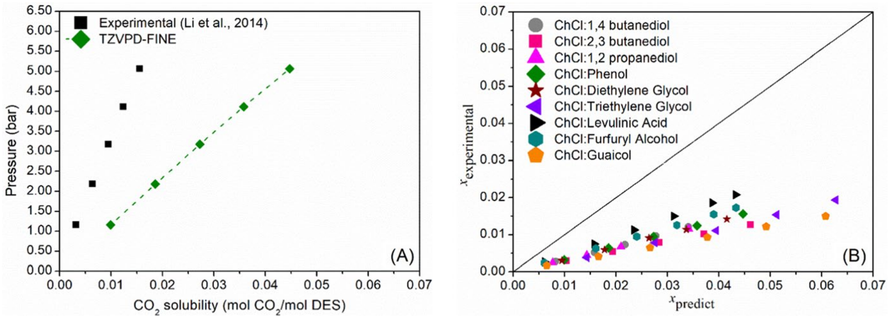

Fig. 2 (A) Comparison between the experimental CO_2 solubility in ChCl:Phenol (1:3 molar ratio) with the COSMO-RS predictions; (B) experimental x_{CO2} vs. predicted x_{CO2} with COSMO-RS for all studied ESs at 1:3 molar ratio

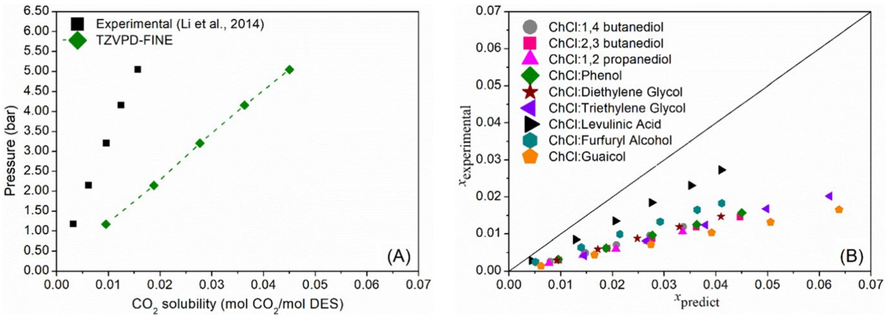

Fig. 3 (A) Comparison between the experimental CO_2 solubility in ChCl:Phenol (1:4 molar ratio) with the COSMO-RS predictions; (B) experimental x_{CO2} vs. predicted x_{CO2} with COSMO-RS for all studied ESs at 1:4 molar ratio

Once again, it is possible to compare the predicted CO_2 solubility in ChCl:Phenol with COSMO-RS to the results obtained in our previous work [46] with CPA and Peng–Robinson EoSs, at 1:3 molar ratio, 313.15 K, and 3 bar. At those conditions, the COSMO-RS model shows an ARD of 187%, whereas ARDs of 6% and 4% were obtained with CPA and Peng–Robinson EoS, respectively. Moreover, the solubility predictions obtained in this work are closer to the experimental values than those obtained by [41] with COSMO-RS for all ESs and pressures at a 1:3 molar ratio (HBA:HBD).

3.3 CH_4 Solubility in ESs at 1:1 Molar Ratio

Experimental and thermodynamic studies on CH_4 solubility in ESs are scarce in the literature [21, 43, 66, 69]. Consequently, a few ESs have been studied for this application in a limited range of molar ratios. In this work, the solubilities of CH_4 in ESs composed of choline chloride as HBA and lactic acid, malonic acid, or phenylacetic acid as HBD (at 1:1 molar ratio) were predicted at 298.15 K, in the pressure range (0.05–50) bar. The results are summarized in Tables S26–S28 and Figure S4 of the

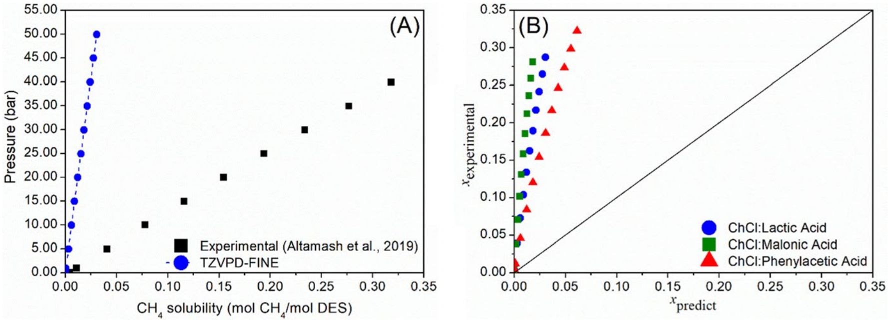

Fig. 4 (A) Comparison of the experimental solubility of CH_4 in ChCl:Lactic Acid (1:1 molar ratio) with the COSMO-RS predictions; (B) experimental x_{CO2} vs. x_{CO2} predicted with COSMO-RS for all studied ESs at 1:1 molar ratio

Supplementary Information and compared to the experimental data available in the literature [69] in Fig. 4(A).

In this scenario, COSMO-RS underestimates the solubility data by one or two orders of magnitude, generally resulting in ARDs larger than 80%. Despite the large deviations, the predicted curves suggest that the solubility increases as the pressure increases, which is confirmed by the experimental data. Regarding the CH_4 absorption performance, the experimental solubility data exhibit the following order: ChCl:Lactic acid > ChCl:Phenylacetic acid > ChCl:Malonic acid due to the C−OH···CH_4 or C=O···CH_4 interactions [21]. Although COSMO-RS confirms that the ES with malonic acid delivers the lowest solubility data, the model suggests that ChCl:Phenylacetic acid would present a higher CH_4 solubilization capacity than ChCl:Lactic acid in the studied conditions.

Although Altamash et al. [69] did not attempt to model the CH_4 solubility data in the ChCl-based ESs, Haider and Kumar [21] modeled the CH_4 solubility in ESs composed of tetrabutylammonium bromide (TBAB):2-methylaminoethanol (MAE), benzyltriethylammonium chloride (BTEACl):MAE, TBAB:2-ethylaminoethanol (EAE), and BTEACl:EAE using NRTL model and Peng–Robinson EoS. Authors observed that both models fit well with the experimental results; however, the NRTL model performed slightly better than the Peng–Robinson EoS. Therefore, classical thermodynamic modeling again represented the experimental data better than COSMO-RS.

3.4 CO_2, CH_4, and H_2S Solubilities in ChCl:Urea at Different Molar Ratios

Experimental solubility data of other gases, such as H_2S, HCl, N_2, and SO_2, in ESs are scarce in the literature [43, 66, 76–88]. Nonetheless, studies addressing modeling, prediction, or molecular dynamics-based strategies to obtain such data are even rarer. Only one study used COSMO-RS to predict the CO_2, CH_4, and H_2S solubilities in ChCl:Urea at different temperatures than 313.15 K was found [43]. In the present study, COSMO-RS was applied to represent the solubility of H_2S, CO_2, and CH_4 in ChCl:Urea in three different molar ratios (1:1.5, 1:2, and 1:2.5), at 313.15 K,

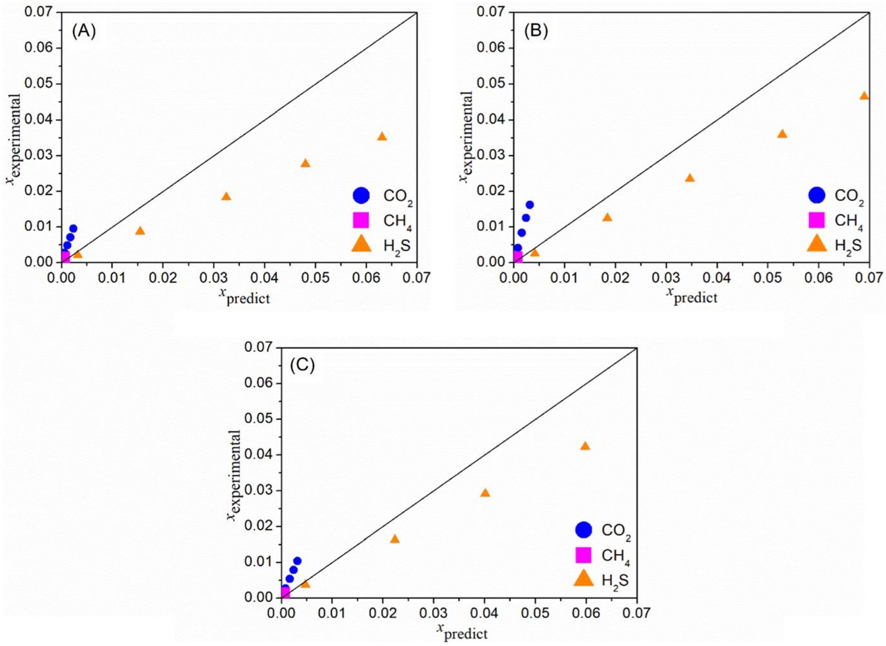

Fig. 5 Comparison between the experimental CO_2, CH_4, and H_2S solubility data with the predicted values with COSMO-RS in ChCl:Urea at (A) 1:2.5 molar ratio (HBA:HBD); (B) 1:1.5 molar ratio (HBA:HBD); and (C) 1:2 molar ratio (HBA:HBD)

and in the pressure range varying between 0.1 and 2 bar. The results are compared with the experimental data measured by Liu et al. [66] in Fig. 5 and Tables S5–S7 and S29–S34 of the Supplementary Information.

In most cases, the model can predict the correct order of magnitude of the solubility data, presenting ARDs varying between 37% and 81%. The smallest deviations were found for the H_2S solubilities (37% < ARD < 72%), whereas ARDs superior to 71% were obtained for CO_2. In general, COSMO-RS underestimates the solubility values of CO_2 and CH_4 (Fig. 5), diverging from the data analyzed by Kamgar et al. [43]. In contrast, the opposite behavior was registered for H_2S.

Unlike the previous cases, COSMO-RS adequately estimates the experimental solubility order for the ChCl:Urea ES: $H_2S > CO_2 > CH_4$. This behavior was expected since H_2S forms stronger hydrogen bonds with ChCl:Urea than CO_2, while CH_4, a rigid and inert molecule, presents only weak van der Waals interactions. The strengths of site-to-site interaction for H_2S, which is much stronger than for CO_2 and CH_4, follow the sequence of Cl (ChCl)–H (H_2S) > O (Urea)–-H (H_2S) > O (ChCl)–H (H_2S) > N (Urea)–-H (H_2S) > H (ChCl)–S (H_2S) > H (urea)–S (H_2S) > N (ChCl)–H (H_2S) [66].

Regarding the absorption capacity at different molar ratios, for H_2S both COSMO-RS and experimental data followed the order 1:1.5 > 1:2 > 1:2.5. These results are not similar to those found in the literature [66] as generally increasing the HBD molar ratio leads to an increase in the gas solubility. On the other hand, CO_2 and CH_4 experimental solubility data follow the order 1:2 > 1:1.5 ≈ 1:2.5, slightly different from that predicted by COSMO-RS (1:2 ≈ 1:1.5 > 1:2.5). Different from the H_2S, where absorption is governed by weak site-to-site interactions, the solubilization of CO_2 and CH_4 in mixtures of ChCl:Urea is driven by the solvent-free volume [66, 89]. Since ChCl:Urea at a 1:2 molar ratio forms a DES (i.e., its melting point is lower than those of 1:1.5 and 1:2.5 molar ratios), a tight aggregation of the molecules is promoted, and the extra free volume favors the gas absorption [66, 89].

3.5 Correction for CO_2 and CH_4 COSMO-RS Predicted Solubilities

The preceding sections have demonstrated the feasibility of conducting a qualitative analysis for ES pre-screening to identify good absorbers for the greenhouse gases addressed in this study. Regrettably, the large deviations between the experimental solubility of GHGs and COSMO-RS predictions limit the application of the model for more quantitative purposes. Following the idea proposed by Liu et al. [41, 90], a systematic correction for the predicted solubilities with COSMO-RS is proposed to improve the accuracy of the solubility predictions. For each ES listed in Table 1, the following temperature–pressure-dependent correlation was applied:

$$\ln x_{\mathrm{CO_2/CH_4}}^{\mathrm{correction}} = \ln x_{\mathrm{CO_2/CH_4}}^{\mathrm{COSMO-RS}} - A \times \frac{1}{T} + BP + C, \tag{5}$$

where $x_{\mathrm{CO_2/CH_4}}^{\mathrm{correction}}$ is the corrected solubility, $x_{\mathrm{CO_2/CH_4}}^{\mathrm{COSMO-}RS}$ is the COSMO-RS predicted solubility value, T is the temperature in Kelvin, P is the pressure in kPa, and A (K), B (kPa^{-1}) and C are fitted parameters for each of the studied ESs.

The parameters A, B, and C were adjusted using the experimental CO_2 or CH_4 solubility values collected from the literature and listed in Table 1. Whenever possible, experimental solubility data obtained in different molar ratios for the common ES were included in the fitting. The correction equations are presented in Table 3, along with the ARDs obtained before and after the correction. Fig. 6 shows the big picture by comparing COSMO-RS corrected solubilities with the experimental values. The corrected solubility values and the corresponding relative deviations are included in Tables S1–S4 and S8–S28 of Supplementary Information.

The ARDs listed in Table 3 show that a much better description of the solubility values is achieved using the temperature–pressure-dependent correction proposed in Eq. 5. For CO_2, the global ARD reduced from 156% to 15% by applying the correction, while a much lower global ARD (11%) was obtained for CH_4 after the correction compared to the value obtained with COSMO-RS (143%). After applying the correction, ARDs lower than 12% were achieved for 12 of the 15 cases analyzed in Table 3, suggesting that the proposed approach offers a good global representation of the CO_2 and CH_4 solubilities. The best results were obtained for CO_2 + ChCl:1,4−butanediol ($\mathrm{ARD_{Corrected}} = 1.1\%$), whereas the outlier system for the two investigated scenarios is CO_2 + ChCl:Guaiacol ($\mathrm{ARD_{COSMO\text{-}RS}} = 302.4\%$; $\mathrm{ARD_{Corrected}} = 73.0\%$). In summary, COSMO-RS can describe most of the solubility trends studied in this work, while the proposed approach for correcting COSMO-RS solubility predictions is a reliable alternative to obtain more accurate results.

Table 3 Corrected COSMO-RS for predicting CO_2 and CH_4 solubilities in the 15 ESs studied in this work

Gas + ES	Correction equation	ARD (%)	
		Before correction	After correction
CO_2 + ChCl:Ethylene Glycol	$\ln x_{CO_2}^{correction} = \ln x_{CO_2}^{COSMO-RS} - 144.85 \times \frac{1}{T} + 1.30 \times 10^{-5} P - 0.77$	33.8	2.1
CO_2 + ChCl:Glycerol	$\ln x_{CO_2}^{correction} = \ln x_{CO_2}^{COSMO-RS} - 473.53 \times \frac{1}{T} - 3.21 \times 10^{-5} P + 1.91$	25.6	1.8
CO_2 + ChCl:Urea	$\ln x_{CO_2}^{correction} = \ln x_{CO_2}^{COSMO-RS} - 218.50 \times \frac{1}{T} - 1.34 \times 10^{-4} P + 2.65$	58.3	10.1
CO_2 + ChCl:Phenol	$\ln x_{CO_2}^{correction} = \ln x_{CO_2}^{COSMO-RS} - 166.65 \times \frac{1}{T} + 3.04 \times 10^{-4} P - 0.60$	80.7	41.3
CO_2 + ChCl:1,4−butanediol	$\ln x_{CO_2}^{correction} = \ln x_{CO_2}^{COSMO-RS} - 157.77 \times \frac{1}{T} + 2.11 \times 10^{-4} P - 0.64$	192.8	1.1
CO_2 + ChCl: 2,3−butanediol	$\ln x_{CO_2}^{correction} = \ln x_{CO_2}^{COSMO-RS} - 261.47 \times \frac{1}{T} + 1.50 \times 10^{-4} P - 0.37$	260.9	7.6
CO_2 + ChCl:1,2−propanediol	$\ln x_{CO_2}^{correction} = \ln x_{CO_2}^{COSMO-RS} - 265.42 \times \frac{1}{T} + 1.94 \times 10^{-4} P - 0.37$	210.0	4.5
CO_2 + ChCl:Diethylene Glycol	$\ln x_{CO_2}^{correction} = \ln x_{CO_2}^{COSMO-RS} - 265.17 \times \frac{1}{T} + 2.16 \times 10^{-4} P - 0.33$	199.1	3.3
CO_2 + ChCl:Triethylene Glycol	$\ln x_{CO_2}^{correction} = \ln x_{CO_2}^{COSMO-RS} - 268.98 \times \frac{1}{T} + 3.31 \times 10^{-4} P - 0.36$	248.5	8.5
CO_2 + ChCl:Levulinic Acid	$\ln x_{CO_2}^{correction} = \ln x_{CO_2}^{COSMO-RS} - 319.21 \times \frac{1}{T} - 3.71 \times 10^{-5} P + 0.63$	111.3	21.6
CO_2 + ChCl:Furfuryl Alcohol	$\ln x_{CO_2}^{correction} = \ln x_{CO_2}^{COSMO-RS} - 400.93 \times \frac{1}{T} - 1.31 \times 10^{-4} P + 0.52$	152.3	7.8
CO_2 + ChCl:Guaiacol	$\ln x_{CO_2}^{correction} = \ln x_{CO_2}^{COSMO-RS} - 368.89 \times \frac{1}{T} - 1.60 \times 10^{-4} P + 0.75$	302.4	73.0
CH_4 + ChCl:Lactic Acid	$\ln x_{CH_4}^{correction} = \ln x_{CH_4}^{COSMO-RS} - 149.78 \times \frac{1}{T} + 7.11 \times 10^{-6} P + 3.04$	93.1	11.4
CH_4 + ChCl:Malonic Acid	$\ln x_{CH_4}^{correction} = \ln x_{CH_4}^{COSMO-RS} - 73.22 \times \frac{1}{T} + 5.27 \times 10^{-6} P + 3.22$	95.5	11.4
CH_4 + ChCl:Phenylacetic Acid	$\ln x_{CH_4}^{correction} = \ln x_{CH_4}^{COSMO-RS} - 242.20 \times \frac{1}{T} + 2.94 \times 10^{-6} P + 2.65$	85.8	11.4

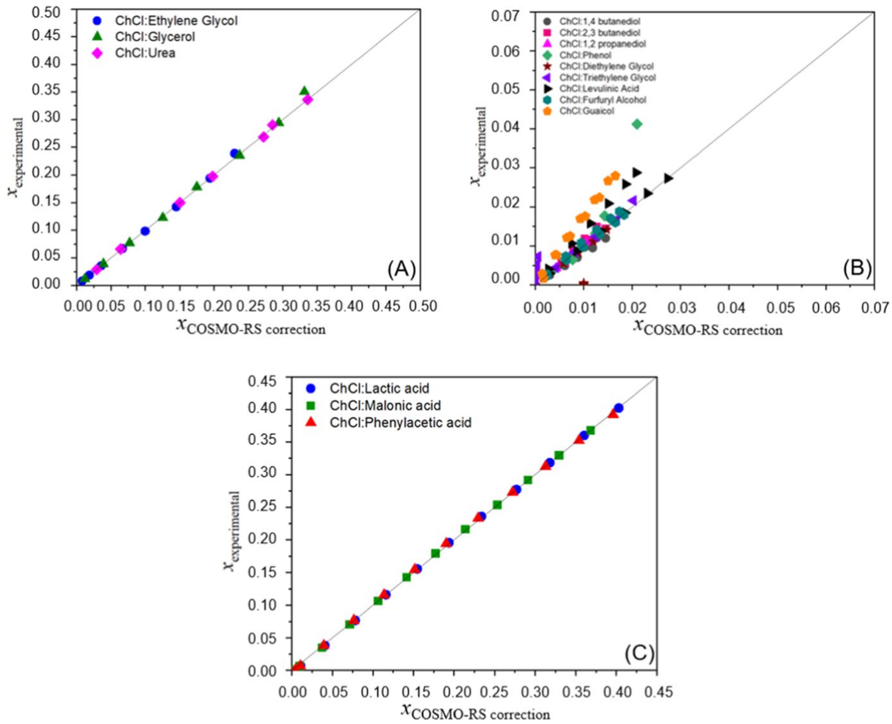

Fig. 6 Comparisonof CO_2 and CH_4 COSMO-RS corrected solubilities with the experimental values for different ESs. The graphs were built following the availability of experimental data in one or more molar ratio for the studied ESs: (A) only for 1:2 molar ratio; (B) 1:2 and/or 1:3 and 1:4 molar ratios; (C) only 1:1 molar ratio

4 Conclusions

In this study, the solubilities of CO_2, CH_4, and H_2S in 17 ChCl-based ESs retrieved from the literature, at 298.15 or 313.15 K and in the pressure range from 1 to 125 bar, were predicted using the COSMO-RS model. In addition, the effect of three different molar ratios of ChCl:urea on the solubility of CO_2, CH_4, and H_2S was investigated. Whenever possible, the results obtained in this study were compared with solubility values estimated in previous works using correlative and predictive thermodynamic models.

In all cases, the deviations obtained with COSMO-RS were larger than those achieved by CPA and Peng–Robinson EoSs, which was expected due to COSMO-RS's fully predictive nature. In most situations, the obtained ARDs were higher than 50%, revealing that COSMO-RS provides only a qualitative picture of the investigated greenhouse gas solubility phenomenon. In a few cases for CO_2 (ChCl:Ethylene Glycol—1:2, ChCl:Glycerol, ChCl:Levulinic acid—1:4) and H_2S (ChCl:Urea—1:1.5 and 1:2), the model offered a more quantitative description of the solubility data, achieving relative deviations inferior to 50%.

The experimental data revealed that an increase in pressure leads to an increase in solubility, which is also captured by the COMOS-RS predictions. The model underestimated the solubility data of CO_2 and CH_4 in ESs with molar ratios of 1:2 and 1:1, respectively. On the contrary, the CO_2 solubilities in 1:3 and 1:4 molar ratios ESs were overestimated by COSMO-RS.

Attempting to achieve a more quantitative description of the solubility data, a correction equation was implemented using temperature–pressure-dependent parameters derived from CO_2 and CH_4 solubility data in ESs. This refined approach significantly improves the accuracy of solubility data, which is reflected by the much lower ARDs obtained for the corrected values compared to predictions directly obtained from COSMO-RS.

This study shows that COSMO-RS is a reliable tool for solvent screening purposes for light gases. Although the model is inadequate for quantitative purposes in many situations, it is suitable for identifying solubility trends in eutectic mixtures, being capable of detecting promising ESs to be further investigated as absorbers in the gas capture field. In contrast, the correlative approach proposed in this work might be employed to obtain more accurate results.

Supplementary Information The online version contains supplementary material available at https://doi.org/10.1007/s10765-024-03363-x.

Acknowledgements The authors thank the São Paulo Research Foundation (FAPESP—2018/19198-9 and 2014/21252-0), Coordination for the Improvement of Higher Education Personnel—Brasil (CAPES)—Finance Code 001, the National Council for Scientific and Technological Development (CNPq—312848/2023-4), and the Fund for the Support of Education, Research and Extension (FAEPEX/UNICAMP) for the financial support. The authors also thank the Human Resources Program of the National Agency of Petroleum, Natural Gas and Biofuels (PRH-ANP). This work was developed within the scope of the project CICECO Aveiro Institute of Materials, UIDB/50011/2020, UIDP/50011/2020 & LA/P/0006/2020, financed by national funds through the FCT/MEC (PIDDAC).

Author Contributions Fernanda Paludetto Pelaquim: Conceptualization, Writing—Original Draft, Validation, Formal analysis, Investigation. Sérgio M. Vilas-Boas: Validation, Formal analysis, Writing—Review & Editing. Débora Costa do Nascimento: Formal analysis, Writing—Review & Editing. Pedro J. Carvalho: Writing—Review & Editing, Resources. Antonio Marinho Barbosa Neto: Writing—Review & Editing. Mariana Conceição da Costa: Supervision, Funding acquisition, Project administration, Writing—Review & Editing.

Data Availability No datasets were generated or analyzed during the current study.

Declarations

Conflict of interest The authors have no conflicts of interest to declare that are relevant to the content of this article.

References

1. C.A. Marques, A.A.S.C. Machado, Found. Chem. **16**, 125 (2014)
2. P. Anastas, N. Eghbali, Chem. Soc. Rev. **39**, 301 (2010)
3. A. Paiva, R. Craveiro, I. Aroso, M. Martins, R.L. Reis, A.R.C. Duarte, ACS Sustain. Chem. Eng. **2**, 1063 (2014)
4. S. Cherukuvada, A. Nangia, Chem. Commun. **50**, 906 (2014)

5. G. García, M. Atilhan, S. Aparicio, Int. J. Greenhouse Gas Control **39**, 62 (2015)
6. M.A.R. Martins, S.P. Pinho, J.A.P. Coutinho, J. Solut. Chem. **48**, 1 (2018)
7. B. Singh, H. Lobo, G. Shankarling, Catal Letters **141**, 178 (2011)
8. Q. Zhang, K. De Oliveira Vigier, S. Royer, F. Jérôme, Chem. Soc. Rev. **41**, 7108 (2012)
9. B. Tang, K.H. Row, Monatsh. Chem. **144**, 1427 (2013)
10. D. Carriazo, M.C. Serrano, M.C. Gutiérrez, M.L. Ferrer, F. del Monte, Chem. Soc. Rev. **41**, 4996 (2012)
11. H. Ghaedi, M. Ayoub, S. Sufian, G. Murshid, S. Farrukh, A.M. Shariff, Int. J. Greenhouse Gas Control **66**, 147 (2017)
12. H. Cheng, Z. Qi, Sep. Purif. Technol. **274**, 119027 (2021)
13. V. Sivabalan, N. Hasnor, B. Lal, Z. Kassim, A.S. Maulud, Appl. Sci. (Switz.) **10**, 25 (2020)
14. D. Lee, W. Go, J. Oh, J. Lee, I. Jo, K.S. Kim, Y. Seo, Chem. Eng. J. **399**, 125830 (2020)
15. Y. Liao, S. Gong, G. Wang, T. Wu, X. Meng, Q. Huang, Y. Su, F. Wu, R.M. Kelly, SSRN Electron. J. **69**, 806–812 (2022)
16. Z. Wang, M. Cheng, J. Bu, L. Cheng, J. Ru, Y. Hua, D. Wang, Adv. Powder Technol. **33**, 103670 (2022)
17. E.L. Smith, A.P. Abbott, K.S. Ryder, Chem. Rev. **114**, 11060 (2014)
18. R. Zhao, D. Pei, P. Yu, J. Wei, N. Wang, D. Di, Y. Liu, J. Sep. Sci. **43**, 348 (2020)
19. F.O. Farias, F.H.B. Sosa, L. Igarashi-Mafra, J.A.P. Coutinho, M.R. Mafra, Fluid Phase Equilib. **448**, 143 (2017)
20. G. Ansarypur, M. Bayareh, A. Jahangiri, J. Therm. Anal. Calorim. **147**, 1689 (2022)
21. M.B. Haider, R. Kumar, Sep. Purif. Technol. **248**, 117055 (2020)
22. A. Tatar, A. Barati-Harooni, A. Najafi-Marghmaleki, A. Bahadori, Int. J. Greenh. Gas Control **58**, 212 (2017)
23. F. Luo, X. Liu, S. Chen, Y. Song, X. Yi, C. Xue, L. Sun, J. Li, ACS Sustain. Chem. Eng. **9**, 10250 (2021)
24. O. Alioui, Y. Benguerba, I.M. Alnashef, J. Mol. Liq. **307**, 113005 (2020)
25. International Energy Agency, Global Energy Review: CO2 Emissions in 2021 Global Emissions Rebound Sharply to Highest Ever Level (2022).
26. D.A. Lashof, D.R. Ahuja, Nature **344**, 529 (1990)
27. M. Höök, X. Tang, Energy Policy **52**, 797 (2013)
28. G. García, S. Aparicio, R. Ullah, M. Atilhan, Energy Fuels **29**, 2616 (2015)
29. G. Luderer, V. Bosetti, M. Jakob, M. Leimbach, J.C. Steckel, H. Waisman, O. Edenhofer, Clim. Change **114**, 9 (2012)
30. F. Petrakopoulou, G. Tsatsaronis, Energy Fuels **28**, 5327 (2014)
31. J. de Riva, J. Suarez-Reyes, D. Moreno, I. Díaz, V. Ferro, J. Palomar, Int. J. Greenh. Gas Control **61**, 61 (2017)
32. Y. Wang, L. Zhao, A. Otto, M. Robinius, D. Stolten, Energy Procedia **114**, 650 (2017)
33. F.P. Pelaquim, A.M.B. Neto, I.A.L. Dalmolin, M.C. da Costa, Ind. Eng. Chem. Res. **1**, 00947 (2021)
34. X. Liu, B. Gao, Y. Jiang, N. Ai, D. Deng, J. Chem. Eng. Data **62**, 1448 (2017)
35. H. Ghaedi, M. Ayoub, S. Sufian, A.M. Shariff, S.M. Hailegiorgis, S.N. Khan, J. Mol. Liq. **243**, 564 (2017)
36. N. Ramzan, M. Rizwan, M. Zaman, M. Adnan, A. Ullah, A. Gungor, U. Shakeel, A. ul Haq, Int. J. Energy Res. **46**, 23775–23795 (2022)
37. K.H. Smith, H.E. Ashkanani, B.I. Morsi, N.S. Siefert, Int. J. Greenh. Gas Control **118**, 103694 (2022)
38. G. Siani, M. Tiecco, P. Di Profio, S. Guernelli, A. Fontana, M. Ciulla, V. Canale, J. Mol. Liq. **315**, 1 (2020)
39. H. Qin, Z. Song, H. Cheng, L. Deng, Z. Qi, J. Mol. Liq. **326**, 1 (2021)
40. X. Liu, Q. Ao, S. Shi, S. Li, Mater. Res. Express **9**, 015504 (2022)
41. Y. Liu, H. Yu, Y. Sun, S. Zeng, X. Zhang, Y. Nie, S. Zhang, X. Ji, Front. Chem. **8**, 1 (2020)
42. J. Wang, Z. Song, L. Chen, T. Xu, L. Deng, Z. Qi, Green Chemical Eng. **2**, 431 (2021)
43. A. Kamgar, S. Mohsenpour, F. Esmaeilzadeh, J. Mol. Liq. **247**, 70 (2017)
44. R. Haghbakhsh, S. Raeissi, J. Chem. Eng. Data **63**, 897 (2017)
45. R. Haghbakhsh, M. Keshtkar, A. Shariati, S. Raeissi, J. Mol. Liq. **330**, 1 (2021)
46. F.P. Pelaquim, R.G. Bitencourt, A.M.B. Neto, I.A.L. Dalmolin, M.C. da Costa, Process. Saf. Environ. Prot. **163**, 14 (2022)
47. F. Rabhi, F. Mutelet, H. Sifaoui, J. Chem. Eng. Data **66**, 702 (2021)
48. M.B. Haider, D. Jha, R. Kumar, M. Sivagnanam, Int. J. Greenh. Gas Control **92**, 1 (2020)
49. A. Klamt, J. Phys. Chem. **99**, 2224 (1995)

50. A. Klamt, V. Jonas, T. Bürger, J.C.W. Lohrenz, J. Phys. Chem. A **102**, 5074 (1998)
51. F. Eckert, A. Klamt, AIChE J. **48**, 369 (2002)
52. H. Cheng, C. Liu, J. Zhang, L. Chen, B. Zhang, Z. Qi, Chem. Eng. Process. **125**, 246 (2018)
53. K.A. Kurnia, S.P. Pinho, J.A.P. Coutinho, Ind. Eng. Chem. Res. **53**, 12466 (2014)
54. K. Paduszyński, Phys. Chem. Chem. Phys. **19**, 11835 (2017)
55. T. Aissaoui, I.M. AlNashef, Int. J. Chem. Mol. Eng. **11**, 54007 (2017)
56. K. Xin, F. Gallucci, M. van Sintannaland, ACS Sustain. Chem. Eng. **10**, 15284 (2022)
57. Z. Song, X. Hu, H. Wu, M. Mei, S. Linke, T. Zhou, Z. Qi, K. Sundmacher, ACS Sustain. Chem. Eng. **8**, 8741 (2020)
58. H. Qin, Z. Song, H. Cheng, L. Deng, Z. Qi, J. Mol. Liq. **326**, 115292 (2021)
59. A. Al-Bodour, N. Alomari, S. Aparicio, M. Atilhan, J. Mol. Liq. **390**, 123114 (2023)
60. M. Mohan, O. Demerdash, B.A. Simmons, J.C. Smith, M.K. Kidder, S. Singh, Green Chem. **25**, 3475 (2023)
61. R.B. Leron, M.H. Li, Thermochim. Acta **551**, 14 (2013)
62. R.B. Leron, M.H. Li, J. Chem. Thermodyn. **57**, 131 (2013)
63. Y. Ji, Y. Hou, S. Ren, C. Yao, W. Wu, Fluid Phase Equilib. **429**, 14 (2016)
64. G. Li, D. Deng, Y. Chen, H. Shan, N. Ai, J. Chem. Thermodyn. **75**, 58 (2014)
65. X. Li, M. Hou, B. Han, X. Wang, L. Zou, J. Chem. Eng. Data **53**, 548 (2008)
66. F. Liu, W. Chen, J. Mi, J.Y. Zhang, X. Kan, F.Y. Zhong, K. Huang, A.M. Zheng, L. Jiang, AIChE J. **65**, 1 (2019)
67. Y. Chen, N. Ai, G. Li, H. Shan, Y. Cui, D. Deng, J. Chem. Eng. Data **59**, 1247 (2014)
68. M. Lu, G. Han, Y. Jiang, X. Zhang, D. Deng, N. Ai, J. Chem. Thermodyn. **88**, 72 (2015)
69. T. Altamash, A.I. Amhamed, S. Aparicio, M. Atilhan, Ind. Eng. Chem. Res. **58**, 8097 (2019)
70. B. COSMOtherm, *Release 2021* (2021).
71. C. Steffen, K. Thomas, U. Huniar, A. Hellweg, O. Rubner, A. Schroer, J. Comput. Chem. **31**, 2967 (2010)
72. M. Diedenhofen, A. Klamt, Fluid Phase Equilib. **294**, 31 (2010)
73. B. COSMOtherm, *Reference Manual* (2021).
74. L. Moity, M. Durand, A. Benazzouz, C. Pierlot, V. Molinier, J.M. Aubry, Green Chem. **14**, 1132 (2012)
75. Y. Liu, Z. Dai, Z. Zhang, S. Zeng, F. Li, X. Zhang, Y. Nie, L. Zhang, S. Zhang, X. Ji, Green Energy Environ. **6**, 314 (2021)
76. J. Zhu, H. Shao, L. Feng, Y. Lu, H. Meng, C. Li, J. Mol. Liq. **341**, 116928 (2021)
77. P. Zhang, W. Xiong, M. Shi, Z. Tu, X. Hu, X. Zhang, Y. Wu, Chem. Eng. J. **438**, 135626 (2022)
78. D. Yang, M. Hou, H. Ning, J. Zhang, J. Ma, G. Yang, B. Han, Green Chem. **15**, 2261 (2013)
79. X. Liu, B. Gao, D. Deng, Sep. Sci. Technol. (Phila.) **53**, 2150 (2018)
80. J. Zhang, L. Yu, R. Gong, M. Li, H. Ren, E. Duan, Energy Fuels **34**, 47 (2020)
81. X. Yang, Y. Zhang, F. Liu, P. Chen, T. Zhao, Y. Wu, Sep. Purif. Technol. **250**, 1 (2020)
82. S. Sun, Y. Niu, Q. Xu, Z. Sun, X. Wei, Ind. Eng. Chem. Res. **54**, 8019 (2015)
83. S. Hou, C. Zhang, B. Jiang, H. Zhang, L. Zhang, N. Yang, N. Zhang, X. Xiao, X. Tantai, ACS Sustain. Chem. Eng. **8**, 16241 (2020)
84. Y. Chen, B. Jiang, H. Dou, L. Zhang, X. Tantai, Y. Sun, Energy Fuels **32**, 10737 (2018)
85. D. Deng, X. Liu, B. Gao, Ind. Eng. Chem. Res. **56**, 13850 (2017)
86. G. Cui, J. Liu, S. Lyu, H. Wang, Z. Li, J. Wang, ACS Sustain Chem Eng **7**, 14236 (2019)
87. X. Wu, R. Guan, W.T. Zheng, K. Huang, J. Taiwan Inst. Chem. Eng. **119**, 45 (2021)
88. D. Deng, C. Zhang, X. Deng, L. Gong, Energy Fuels **34**, 665 (2020)
89. A.P. Abbott, G. Capper, D.L. Davies, R.K. Rasheed, V. Tambyrajah, R. Soc. Chem. **70**, 71 (2003)
90. X. Liu, T. Zhou, X. Zhang, S. Zhang, X. Liang, R. Gani, G.M. Kontogeorgis, Chem. Eng. Sci. **192**, 816 (2018)

Authors and Affiliations

Fernanda Paludetto Pelaquim[1] · Sérgio M. Vilas-Boas[1] · Débora Costa do Nascimento[1] · Pedro J. Carvalho[2] · Antonio Marinho Barbosa Neto[3] · Mariana Conceição da Costa[1]

✉ Mariana Conceição da Costa
mcosta@unicamp.br

1 School of Chemical Engineering, University of Campinas – UNICAMP, 500 Albert Einstein Avenue, Campinas, SP 13083-852, Brazil

2 Department of Chemistry, CICECO − Aveiro Institute of Materials, University of Aveiro, 3810-193 Aveiro, Portugal

3 ThermoPhase, Petroleum Engineering Department, State University of Santa Catarina – UDESC, Avenida Lourival Cesário Pereira, Balneário Camboriú, SC 88336-275, Brazil